

ARTICLE

Individual-Based Modeling of Delta Smelt Population Dynamics in the Upper San Francisco Estuary III. Effects of Entrainment Mortality and Changes in Prey

Wim J. Kimmerer*

Romberg Tiburon Center for Environmental Studies, San Francisco State University, 3150 Paradise Drive, Tiburon, California 94920, USA

Kenneth A. Rose

Horn Point Laboratory, University of Maryland Center for Environmental Science, Post Office Box 775, Cambridge, Maryland 21613, USA

Abstract

We used an individual-based model, developed previously for the endangered, endemic Delta Smelt *Hypomesus transpacificus*, to investigate two factors widely believed to affect its abundance in the San Francisco Estuary: entrainment in large water diversion facilities and declines and species shifts in their zooplankton prey. Previous analyses suggested that these factors had substantial effects on the Delta Smelt population, although evidence is accumulating that other factors, such as contaminants and predation, are also having effects. Simulations were performed for 1995–2005 with either entrainment mortality set to zero or zooplankton biomasses replaced with values sampled from pre-decline years. The detailed individual-based and spatial model output was summarized as the annual finite population growth rate (λ). Eliminating entrainment mortality increased the geometric mean λ by 39% through increased survival of larvae and adults. Substituting historical food for present-day food resulted in variable annual λ values with a geometric mean that was 41% greater than the baseline value (14–81% across 10 alternative food scenarios). Historical food caused higher juvenile consumption and growth rates, leading to larger recruits, earlier maturity, and higher individual fecundity. These results were robust to four sets of simulations using alternative formulations for density dependence, mortality, maturity, and larval growth.

Natural populations are subject to myriad environmental influences whose effects can be difficult to distinguish (Gunderson and Leal 2016). Identifying influences on endangered species is particularly challenging because of low population size and restrictions on sampling. This problem is particularly acute with the Delta Smelt *Hypomesus transpacificus*, which is endemic to the San Francisco Estuary (SFE). The Delta Smelt is listed by the State of California as endangered and is listed by the federal government (U.S. Fish and Wildlife Service) as

threatened but warranted for endangered status. Abundances of Delta Smelt and three other pelagic fishes declined sharply around 2002 (Sommer et al. 2007; Thomson et al. 2010), and the ensuing conflicts over causes and remedies have been intense (Hanak et al. 2008).

Various mechanisms for the decline and continued low abundance of Delta Smelt have been proposed and supported with evidence (IEP-MAST 2015). Two mechanisms with substantial statistical support are the focus of this paper. First, the SFE is atypical in having large quantities

*Corresponding author: kimmerer@sfsu.edu
Received October 1, 2017; accepted November 20, 2017

of freshwater diverted from the tidal freshwater reach, carrying organisms (e.g., phytoplankton; Jassby et al. 2002) entrained with the diverted water. Although salvage facilities are intended to extract fish from the diverted water, poor survival within the diversion facilities and in waterways leading to the facilities produces diversion-related mortality (Castillo et al. 2012). This mortality has been partly implicated in the declines of several species, including the Delta Smelt (Moyle et al. 1992; Bennett 2005; Kimmerer 2008, 2011). However, this mortality is difficult to quantify because of the spatial complexity of the estuary, the temporal variability of the flow field, and the difficulty of tracking abundance of rare fish, even with a massive sampling effort (IEP-MAST 2015). Though the degree of entrainment mortality has been disputed (Kimmerer 2011; Miller 2011; Miller et al. 2012), the intense management focus on reducing entrainment mortality (Brown et al. 2008; USFWS 2008) was a key impetus for using a model to examine the population-level effects of entrainment mortality.

Second, a sharp decline in abundance of copepods—the principal prey of Delta Smelt—in the late 1980s (Kimmerer et al. 1994) was followed by indications of food limitation in Delta Smelt. These included a decline in mean Delta Smelt size (Bennett 2005), a high frequency of empty guts (Slater and Baxter 2014), low glycogen content in livers (Bennett 2005; Hammock et al. 2015), and correlations of survival indices to zooplankton abundance (Bennett 2005; Kimmerer 2008).

Several studies have applied statistical models to examine potential causes of the decline in Delta Smelt (Bennett 2005; Mac Nally et al. 2010; Thomson et al. 2010; Feyrer et al. 2011; Maunder and Deriso 2011). Although informative, these studies were based on aggregated indices of population abundance. Delta Smelt and their prey live in a moving, dispersive frame of reference in which the factors that are likely to influence the population vary both temporally and spatially. Spatial patterns of habitat use and the joint distributions of stressors and mobile organisms (including Delta Smelt and their prey) are important for understanding population declines and for conservation (Ward et al. 2012). A rich monitoring data set (e.g., >300,000 samples of fish and >21,000 samples of zooplankton; Merz et al. 2011) allows for explicit representation of the spatiotemporal dynamics of environmental influences and Delta Smelt distribution, providing for additional insights into the causes of decline and the prospects for recovery.

We took advantage of the rich data set on Delta Smelt to develop (Rose et al. 2013a, 2013b) and apply (this paper) a spatially explicit individual-based model (IBM). This modeling effort was intended as a complement to the more aggregated statistical analysis (e.g., Thomson et al. 2010) and life cycle modeling (Maunder and Deriso 2011)

to assess how losses of Delta Smelt in the water diversion facilities (entrainment) and declines in food availability may have affected the population growth rate. Simulations were performed for 1995–2005 either with entrainment mortality eliminated or with zooplankton biomass replaced with values from pre-decline years. Model predictions were compared using the annual finite population growth rate (λ) and detailed output on individuals to assess the importance of these two factors in the decline of Delta Smelt. Although other factors may have contributed to the decline (e.g., contaminants, predation, and turbidity; see Discussion), the strong scientific and management interest in entrainment mortality and food limitation led us to focus on their relative contributions.

METHODS

Study site and species.—The SFE is a highly altered and managed ecosystem (Nichols et al. 1986; Cloern and Jassby 2012). The climate is Mediterranean; most precipitation occurs from about November to April, with very high interannual variability. Freshwater flow is positively related to the abundance of some species of fish and crustaceans (Jassby et al. 1995), while flow effects on lower trophic levels are mixed (Jassby et al. 2002; Kimmerer 2002). The northern portion of the estuary is mesotidal, river-dominated, and turbid. This area includes the California Delta (hereafter, Delta), a network of tidal channels formed by the confluence of the Sacramento and San Joaquin rivers and some smaller rivers. The water diversion facilities are in the southern Delta, where most of the water arrives from the Sacramento River via reverse (southward) net flows in the Old and Middle rivers (Figure 1). Suisun and San Pablo bays are broad, shallow (5-m mean depth), brackish, turbid bays with deep, narrow channels.

Delta Smelt are semi-anadromous, spawning in freshwater and rearing mainly in brackish water (Moyle 2002; Bennett 2005; Sommer et al. 2011). Delta Smelt lay adhesive eggs mainly during March–May in the Delta and Suisun Marsh (Figure 1). Larvae rear in freshwater before most of them move into water with salinity of approximately 0.5–6 (Bennett 2005), roughly where osmoregulatory stress is minimized (Hasenbein et al. 2013). The habitat of juvenile Delta Smelt can be described as open water of low salinity, high turbidity, and temperatures below about 24°C (Feyrer et al. 2007; Nobriga et al. 2008). A contingent of Delta Smelt remains in tidal freshwater within the northern Delta (Sommer and Mejia 2013). Most Delta Smelt reach maturity in 1 year and undergo a diffuse, protracted spawning migration into freshwater (Bennett and Burau 2014). A small proportion of Delta Smelt survive to spawn at an age of 2 years (Bennett 2005). Delta Smelt are planktivorous, feeding mainly

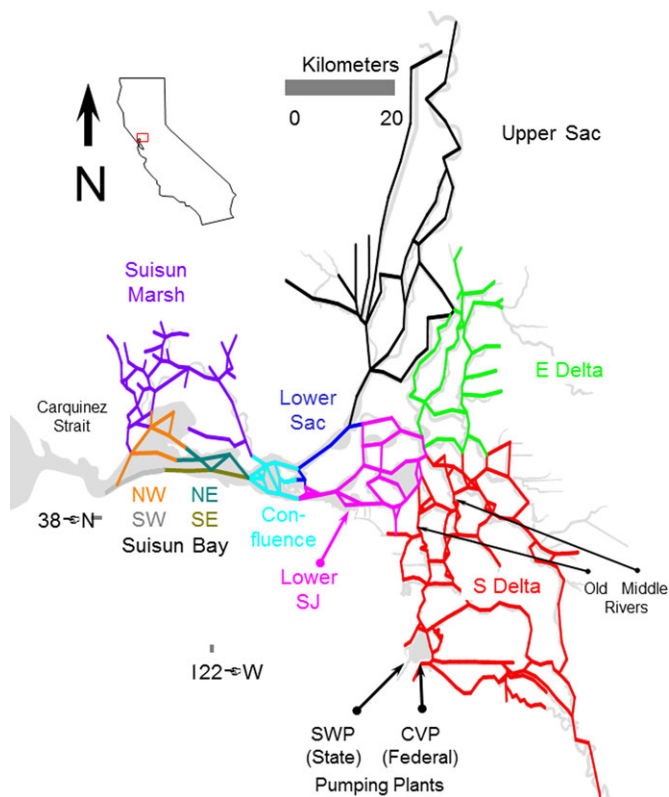


FIGURE 1. Location of the San Francisco Estuary, California, with the model grid and boxes, color-coded with box names, and the locations of diversion pumping plants (Sac = Sacramento River; SJ = San Joaquin River; SWP = State Water Project; CVP = Central Valley Project). Gray represents the outline of the estuary. Boxes are described in more detail by Rose et al. (2013a). [Color figure can be viewed at afsjournals.org.]

on copepods, although larger prey (e.g., amphipods and mysids) are consumed by larger individuals (Slater and Baxter 2014).

Model description.—The IBM was described in detail by Rose et al. (2013a); only features central to this analysis are summarized here and described more fully in the Appendix. The IBM follows the reproduction, growth, mortality, and movement of “super-individuals” (Scheffer et al. 1995) over their entire life cycle. The fish are modeled on a spatial grid representing nearly their entire geographic range by using a one-dimensional channel-node hydrodynamic model both for the grid and to determine transport-based movements of larval Delta Smelt. The grid is nested within a series of 11 spatial boxes (Figure 1). Daily values of salinity and temperature and the means and variances of zooplankton biomass are the same in all channels within a box.

The model is run using historical conditions for 1995–2005, after a 4-year spin-up in which 1999 baseline conditions are repeated. This time period was selected because it encompasses the period of sharp decline in Delta Smelt

abundance and because the environmental and biological data needed for the IBM were relatively complete for this time period (Rose et al. 2013a). Of the many assumptions that went into this model, key assumptions for this analysis are that (1) the principal environmental influences on Delta Smelt are water movement and losses of fish to the diversion facilities, temperature effects on development, and feeding; and (2) the spatial behavior of postlarval fish can be represented by a relatively simple algorithm for swimming behavior that varies with salinity and season (see Appendix).

Traits tracked for each super-individual include life stage, growth rate, weight, length, age, diet, location on the grid, maturity status, fecundity, and worth. Worth, the number of identical individuals represented by a super-individual, is decreased each day to account for mortality and is used to scale output from super-individuals to the population. Super-individuals progress through a series of life stages: egg, yolk-sac larva, larva, postlarva, juvenile, and adult. Development to the next life stage is based on temperature for egg to yolk-sac larva to larva; is based on length for larva to postlarva to juvenile; and is based on date (January 1) for juvenile to age-1 adult and for age-1 to age-2 adult. January 1 was used to mark the birthdays for convenience and because it also corresponded to a low-growth period prior to any possible spawning.

Daily growth rate is determined using a bioenergetics model and depends on body weight, temperature, and feeding rate (Table 1). The feeding rate is a saturating functional response to the summed biomass densities of six food groups (see equation 10 in Rose et al. 2013a), with separate vulnerabilities (0 or 1) and half-saturation constants for each food group and life stage. Biomass of each food group is determined from long-term monitoring data and from available data on carbon per individual.

Movement on the spatial grid is by passive transport using a particle-tracking model (Kimmerer and Nobriga 2008) for yolk-sac larvae, larvae, and postlarvae; for juveniles and adults, movement is modeled as a behavioral response to salinity. Development, reproduction, growth, and mortality are updated daily, while movement of all larval stages is updated hourly and movement of juveniles and adults is updated every 12 h.

Mortality includes a rate that declines with life stage; it is constant within each stage and is the same for all model runs. Daily instantaneous mortality is temperature-dependent for eggs and is set at 0.035 for yolk-sac larvae (calibrated), 0.05 for larvae, 0.03 for postlarvae, 0.015 for juveniles, and 0.006 for adults. Additional mortality results from (1) starvation of fish whose weight goes below half that expected from length and (2) entrainment by the two water diversion facilities (Figure 1). Survival of Delta Smelt trapped at these facilities is low, and the catch at the facilities is a poor measure of entrainment mortality

TABLE 1. Characteristics of zooplankton groups used in model simulations, with dates of introduction, abundance patterns, and distribution from the Interagency Ecological Program's zooplankton monitoring program (Orsi and Mecum 1986; Orsi and Walter 1991; Orsi and Ohtsuka 1999).

Group	Taxa	Introduced	Remarks
1	<i>Limnoithona tetraspina</i>	1993	Most abundant copepod in the low-salinity zone. Small (<0.5-mm) cyclopoid not often consumed by fish, including Delta Smelt (Bryant and Arnold 2007; Slater and Baxter 2014). Most abundant at salinity ~2–8
2	Calanoid copepodites	Some native	Juveniles of all calanoid copepods
3	Other calanoid adults	Some native; others 1978–1993	Includes <i>Acartia</i> spp. and the introduced species <i>Sinocalanus doerri</i> (1978), <i>Tortanus dextrilobatus</i> (1993), and <i>Acartiella sinensis</i> (1993)
4	<i>Acanthocyclops</i>	Presumed native	Freshwater cyclopoid, common at times
5	<i>Eurytemora affinis</i>	Native or introduced before 1972	Important food for small fish (Moyle et al. 1992). Common before 1987 at salinity 0.5–6 (Kimmerer et al. 1998); now abundant in spring but rare in summer–fall
6	<i>Pseudodiaptomus forbesi</i>	1988	Most common food of Delta Smelt in summer–fall (Moyle et al. 1992; Slater and Baxter 2014). Population center in freshwater

(Kimmerer 2008; Castillo et al. 2012). Entrainment mortality was estimated previously from catches of fish in trawl surveys in the south Delta together with flow in the Old and Middle rivers that would transport fish toward the diversion facilities (Kimmerer 2008, 2011).

Entrainment mortality of the three larval stages was modeled by tracking their movements as passive particles. Any larval-stage super-individual that arrived in one of the spatial cells containing a diversion facility was removed from the simulation. This mortality was therefore uncalibrated to previous statistical estimates and arose purely through the transport of particles via the movement of water as represented by the hydrodynamic model.

Entrainment of juveniles and adults was more complicated because their movement did not correspond to movement of the water. Juveniles and adults also occasionally arrived at the diversion facilities and were therefore removed from the simulation. However, many adult Delta Smelt are lost to entrainment in years when net flow is southward toward the diversion facilities (Kimmerer 2008), despite the competence of adult Delta Smelt at moving against the net flow of water (Bennett and Burau 2014). To account for this additional entrainment mortality beyond that due to arrival in a model cell with a diversion, an additional increment of daily mortality to fish in the South Delta model box (Figure 1) was added to their base daily mortality rate. This mortality increment depended on the direction of flow in the Old and Middle rivers (i.e., mortality was incremented when flow was toward the diversion facilities).

The model was calibrated by adjusting two parameters. First, the daily natural mortality of yolk-sac larvae was set so that the mean annual January abundance in the model across all years was close to the historical mean

based on data for the model period (see Rose et al. 2013a). This calibration step included adult entrainment due to transport together with an assumed initial value of the additional mortality rate based on the direction of Old and Middle River flows. We estimated a provisional value of the added mortality term that generated annual numbers of fish entrained consistent with estimates obtained under gross assumptions about the typical duration (d) of pumping and the numbers and fraction vulnerable (i.e., in the South Delta). Once the yolk-sac larval mortality rate was set, we then re-adjusted the value of the additional daily entrainment mortality term so that the mean annual proportion of adults lost to entrainment over the model period matched a corresponding literature-based estimate (Kimmerer 2008; as modified by Kimmerer 2011). This two-step process minimized the risk that the additional mortality term for adult entrainment would be inflated by selecting too low a value of the yolk-sac larval mortality rate (i.e., both targets had to be met simultaneously). No year-specific adjustments were used in the calibration; therefore, the interannual variability in model output was due entirely to variability in time-specific model inputs (i.e., hydrodynamics, temperature, salinity, and food) and the internal dynamics (growth, mortality, reproduction, and movement) of individuals in the modeled population. Rose et al. (2013a) reported that the final calibrated version resulted in an average January adult abundance of 2.7×10^6 (compared to the data-based target of 2.3×10^6) and an average fraction of adults lost to diversions of 11% (the target was 10%). The possible influence of uncertainties in model assumptions and in entrainment is explored in the Discussion.

Model corroboration consisted of then simulating the 1995–2005 period and confirming that the model—

calibrated to overall average conditions only—reasonably generated the year-to-year trend in population abundance (i.e., the decline; see figure 5 in Rose et al. 2013a). We consider this corroboration because we did not attempt to fit to individual years or to the pattern in the time series of annual abundances.

Simulations of eliminating entrainment mortality and historical food.—All simulations for this study were conducted for water year 1995 (i.e., October 1994 through September 1995) to water year 2005. Simulations comprised a sensitivity analysis in which the output of a baseline run, which included the calibrated values of entrainment mortality and food from the model period, was compared with output from runs in which either entrainment mortality was eliminated or food availability was set to historical (pre-decline) conditions. Model results were summarized each year by using the information predicted for individuals to estimate an age-structured matrix projection model; λ was then estimated from the matrix model using eigenvalue analysis (Supplement D in Rose et al. 2013a). All analyses of model output were conducted in R version 3.1.1 (R Development Core Team 2014).

Entrainment mortality in the Delta is the consequence of the movement of water containing fish toward the diversion facilities in the southern Delta. Modeling a cessation of diversion would have required modeling California's complex water management system, in which the Delta is the hub for water routing (Draper et al. 2004). This would have required running a system simulation model under probably unrealistic assumptions about how water would be stored and routed if diversions from the southern Delta were to cease. However, our objective was more modest than this: given today's system configuration and operating procedures, how would the population trajectory change if entrainment mortality was entirely eliminated? This approach established an upper limit to the improvement that would be possible through manipulation of entrainment mortality alone.

Entrainment mortality was eliminated in two steps. First, the added mortality related to Old and Middle River flow was set to zero. Second, super-individuals that arrived at the diversion facilities were saved and moved to a location (grid cell) within the Confluence box (Figure 1) at least a few days' travel from the diversion facilities. Model results were insensitive to the box into which individuals were placed, except that individuals relocated back into the South Delta were often re-entrained; therefore, individuals were not relocated to the South Delta box. In practice, fish that are salvaged from the diversion facilities are moved to the Confluence region to prevent re-entrainment.

Investigating the effects of food required simulations that accounted for movements of fish on the reticulate

spatial grid and for the spatially and temporally variable food supply—both of which defy aggregation into simple annual indices. We therefore substituted zooplankton data from the pre-decline period of 1972–1986 (“historical period”) for data from the period 1995–2005 (“model period”). The purpose was to mimic spatially and temporally variable feeding conditions that existed before the most substantial declines in abundance and shifts in species composition of the zooplankton (Winder and Jassby 2011). This substitution was complicated by the fact that both the Delta Smelt and the zooplankton move with the water, whereas the model and the data have a spatially fixed frame of reference. Furthermore, hydrodynamic model output was not available for the substitute years from the historical period. Finally, zooplankton species composition has changed radically from the historical period to the model period (Table 1). The copepods *Limnoithona tetraspina* and *Pseudodiaptomus forbesi*, each comprising one of the six zooplankton groups included in the model, were not yet present during the historical period. Several other changes in species composition (Table 1) may have altered the feeding environment in ways not reflected in our grouping of zooplankton in the IBM.

To solve the problem of mismatching reference frames, we used the observation that distributions of zooplankton species in salinity space are consistent within a given season and time period and are generally weakly related to other factors (Kimmerer et al. 1998). Therefore, we used the spatial response of estuarine salinity to freshwater flow to determine the historical distributions of zooplankton to use during the model period. To do this, we matched years during the model period with years during the historical period by their hydrology, and we substituted the zooplankton in the model years with zooplankton from the matched historical years. Our assumption was that this would place the zooplankton in the correct position relative to salinity, thereby representing a realistic change relative to any distributional shifts in Delta Smelt. We used two metrics of hydrologic conditions to match each of the model period years to historical years. The first metric was net Delta outflow (m^3/d), defined as the daily flow from the Delta into Suisun Bay (Figure 1), which is estimated from a daily water budget employing the same data used as boundary conditions for the hydrodynamic model. The second metric was the distance (km) up the estuary to where the tidally and daily averaged near-bottom salinity is 2 (“X2” of Jassby et al. 1995); this represents a measure of the physical response of the estuary to freshwater flow. Originally derived by interpolation from continuous monitoring data, X2 is now calculated from the log of outflow by using a time-series model (Jassby et al. 1995). Although X2 is somewhat redundant to outflow, the historical years that matched the model years differed

between the two metrics; because we were unsure which metric was a more accurate approach to match years for zooplankton, we used both metrics.

The year 1978 was eliminated from the matching process. During winter and spring 1978, zooplankton biomass was exceptionally low in areas where adult Delta Smelt were most abundant. This resulted in (1) a simulated mean feeding rate that was only 14% of the maximum during January–February and (2) low reproductive rates and recruitment failure that were not apparent in Delta Smelt data from 1978. In all other historical years, zooplankton biomass supported an adult feeding rate greater than 50% of the maximum. Low food biomass in 1978 appeared to be an artifact of low sampling coverage for zooplankton during that year.

We developed a matrix of the sum of squared differences between the vectors of monthly values of outflow or X2 from each model year and each historical year. The first set of substitute years for outflow or X2 were those with the lowest sum of squared differences, the second set had the next lowest, and so on for a total of five sets of historical years. This process gave five sequences of historical years based on outflow and five sequences based on X2. Zooplankton biomass from each series of years from the historical period was then interpolated and sampled as in the original simulations (Rose et al. 2013a) and was used to replace the zooplankton in the model years (Table 2). An example (Figure 2) shows zooplankton biomass in the Northeast Suisun Bay model box for model year 1999 and for the five historical years with the best match based on X2.

Model experiments and outputs.—Three numerical experiments were performed using the IBM to compare the effects of entrainment mortality and food abundance on the population growth of Delta Smelt. Experiment 1 was designed to compare the effect of eliminating entrainment mortality with that of substituting historical zooplankton for model period zooplankton. The original baseline was run along with a corresponding run in which there was no entrainment mortality; five runs using historical food based on outflow with each of the five sequences of year substitutions; and five runs using historical food based on X2. The analysis focused on comparisons between each of these model runs and the baseline. Most of the detailed results are presented for experiment 1 only.

The baseline was developed through model calibration (Rose et al. 2013a) and is the outcome of decisions about how to represent key life cycle processes in the model. Some of these decisions were rather uncertain because we lacked detailed information. We therefore conducted additional simulations of the baseline using alternative formulations for these processes, and we call these “alternative baselines” (Rose et al. 2013b). Each of the alternative baselines differed from the original baseline by how a

TABLE 2. Years from 1972–1986 used to substitute zooplankton biomass for each year of the model period 1995–2005 (see Methods for definition of X2).

Model year	Year 1	Year 2	Year 3	Year 4	Year 5
Substitutes based on outflow					
1995	1980	1983	1982	1974	1973
1996	1975	1973	1980	1979	1986
1997	1980	1973	1974	1984	1982
1998	1986	1980	1982	1973	1983
1999	1975	1973	1979	1980	1981
2000	1975	1979	1973	1981	1980
2001	1981	1977	1976	1979	1985
2002	1981	1985	1976	1979	1977
2003	1979	1981	1985	1976	1977
2004	1979	1975	1981	1985	1973
2005	1979	1981	1975	1985	1976
Substitutes based on X2					
1995	1982	1980	1986	1983	1975
1996	1975	1980	1986	1982	1973
1997	1973	1980	1982	1974	1984
1998	1982	1983	1980	1975	1986
1999	1975	1973	1980	1974	1982
2000	1986	1979	1980	1981	1975
2001	1981	1979	1985	1986	1976
2002	1979	1981	1985	1980	1976
2003	1980	1979	1981	1986	1973
2004	1980	1979	1986	1981	1973
2005	1980	1979	1986	1975	1981

single process was represented (Table 3): (1) mortality rate during the juvenile life stage was density dependent rather than independent of population size; (2) daily mortality rate was inversely related to length instead of constant within each life stage; (3) larval growth rate was fixed instead of dependent on food supply; and (4) maturity was a smooth function of length instead of a step function.

Rose et al. (2013b) showed that the four alternative baselines generated key model outputs that were qualitatively similar to those from the original baseline. However, quantitative differences in λ values prompted analyses to determine whether the conclusions derived from experiment 1 were robust to the alternative baseline formulations. Experiment 2 repeated the simulations in experiment 1 but with each of the four formulations (subsets 2.1–2.4) used in the alternative baselines (Table 3), resulting in a total of 48 model simulations. These results were compared with those from experiment 1 to determine how model results were affected by the alternative formulations (Table 3). Experiment 3 combined historical food conditions (based on X2 only) with the elimination of

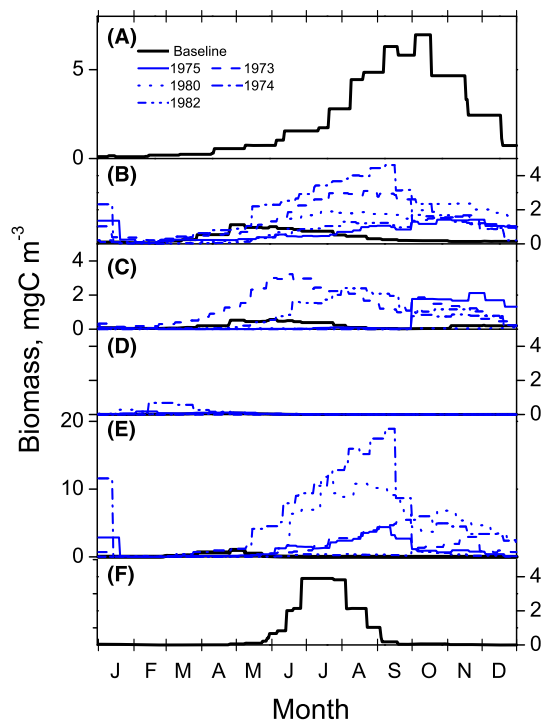


FIGURE 2. Example model inputs for zooplankton biomass (mg C/m^3) during calendar year 1999 in the Northeast Suisun Bay box (Figure 1) and from historical years matched by X2 (defined in Methods). Panels provide data for individual taxa: (A) *Limnithona tetraspina* adults (not present in historical years); (B) calanoid copepodites; (C) calanoid adults not included in other panels; (D) *Acanthocyclops* spp.; (E) *Eurytemora affinis* adults (note the different scale); and (F) *Pseudodiaptomus forbesi* adults (not present in historical years). [Color figure can be viewed at afs.journals.org.]

entrainment mortality to confirm that the effects of historical food and elimination of entrainment mortality were additive (i.e., could be examined separately).

Model comparisons.—The principal metric for comparison among simulations was the annual time series of λ (10 values for the period 1995–2004). The temporal dynamics of λ values showed the same general interannual pattern as adult abundances in January of each year; Rose et al. (2013a; their figure 5) depict and discuss the general agreement between simulated and observed adult abundances. Each simulation was further summarized using the geometric mean of the 10 annual λ values, since these are multiplicative. Several additional model outputs were examined to investigate why the λ values differed among treatments within experiments (Table 4). Most of these results are presented for experiment 1 using historical food based on X2 only, since values using outflow gave broadly similar results. Mean length and weight of recruits (new age-1 fish on January 1) were computed as measures of individual growth during the first year of life. Length is positively related to reproductive success in the model because both maturity and fecundity depend on length

and because larger fish are more likely to spawn a second time. Stage-specific survival fractions and average durations provide information on which life stages responded to elimination of entrainment mortality and substitution with historical food. Average stage duration is a measure of growth rate for feeding stages whose durations are defined by length (i.e., larvae and postlarvae).

We examined growth responses by calculating the proportion of maximum consumption rate (C/C_{max} ; hereafter, “ P -value”) realized by individuals in each of the feeding life stages and comparing it among simulations within each experiment. The P -values were determined for each Delta Smelt life stage from the densities of the six zooplankton groups through the multispecies functional response (Rose et al. 2013a).

Geometric mean values of λ were further compared in experiments 1 and 3 to determine whether the effects of eliminating entrainment and using historical food were independent. We computed the products of the geometric means from the simulation with no entrainment mortality and present-day food and from each of the five simulations with entrainment mortality and historical food from experiment 1. These would be close to values from experiment 3 (and their ratios would be close to 1.0) if the effects of entrainment and historical food acted independently within the model.

RESULTS

Entrainment Mortality Eliminated

In experiment 1, eliminating entrainment mortality increased λ in all years (Figure 3A). Experiment 2 (alternative formulations; Table 3) gave results for entrainment mortality similar to those of experiment 1 (Figure 3B–E). The original baseline had a geometric mean λ of 0.90, while the geometric mean value of λ varied from 0.75 to 0.94 among the four alternative baselines in experiment 2 (second column in Figure 4; Table 5). With entrainment mortality eliminated, the geometric mean λ was 40% higher than baseline in experiment 1 and 30–42% higher than baseline in experiment 2.

The effect of entrainment mortality was greater during the latter half of years in the model run, partly because poor feeding conditions led to slower development of the larval stages, extending the period of high vulnerability to water diversion (Figure 5A–D). During 1996–2000, young-of-the-year survival was on average 10% higher and adult survival was on average 15% higher without entrainment mortality than with entrainment mortality (Table 6; Figure 5). During 2001–2005, these values increased to 19% and 28%, respectively. Thus, particularly in the latter period, rather modest differences in daily mortality accumulated to produce substantial differences in survival

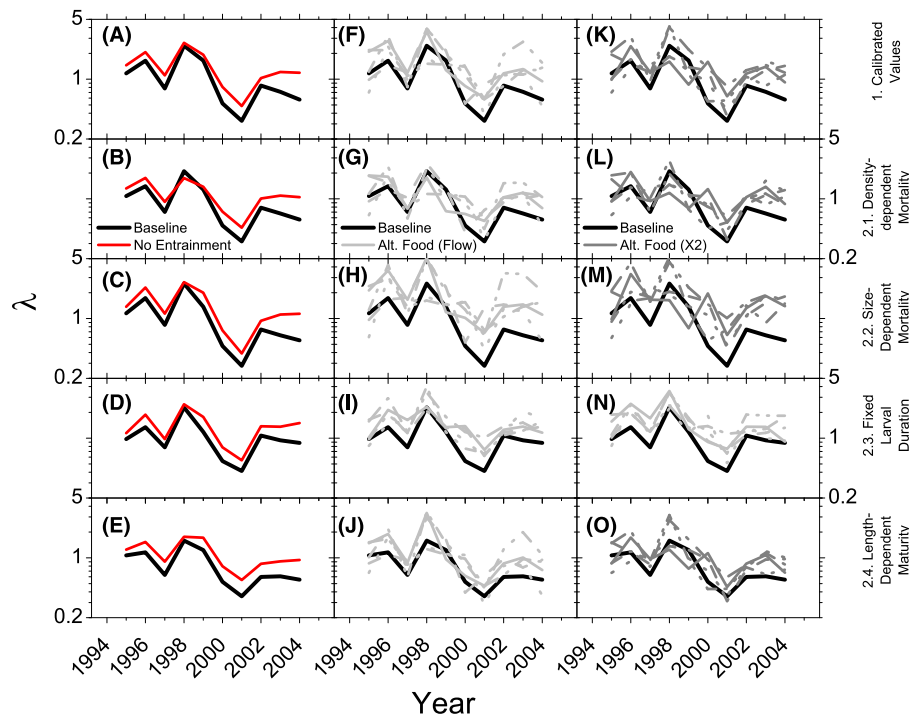


FIGURE 3. Model time series of the annual finite population growth rate (λ) for Delta Smelt in each set of 12 simulations from experiments 1 and 2 (listed on the right side; experiment 2 subsets are defined in Table 3). Each panel contains the baseline value (thick line) and (A)–(E) values obtained under zero entrainment mortality (thin line); (F)–(J) values obtained from five runs with historical food based on outflow (alternative [Alt.] food; thin lines); or (K)–(O) values obtained from five runs with historical food based on X2 (thin lines; X2 is defined in Methods). [Color figure can be viewed at afs.journals.org.]

TABLE 3. Alternative formulations for key processes that defined the alternative baselines (Rose et al. 2013b) used in experiment 2 compared with their formulations in the original baseline used in experiment 1 for Delta Smelt.

Subset	Name	Baseline function	Alternative function	Reason for modification
2.1	Density-dependent mortality	Density independent at all life stages	Juvenile daily mortality increased exponentially with density in a spatial box (see equation 2 in Rose et al. 2013b)	Evidence for density dependence at large population size (Bennett 2005; Maunder and Deriso 2011)
2.2	Size-dependent mortality	Mortality decreases stepwise by life stage	Decreasing as a power function of length (see equation 1 in Rose et al. 2013b)	Stepwise decrease in mortality may be too crude to realistically represent the size dependence of predation
2.3	Fixed larval growth	Determined by food and bioenergetics	Fixed stage duration of 26 d from average over years in simulations of the original baseline	Uncertainty about larval feeding and bioenergetics, especially under historical food conditions
2.4	Length-dependent maturity	Fish larger than 60 mm are mature	Fraction mature varies smoothly with length around 60 mm (see Figure 3 in Rose et al. 2013b)	Model results were sensitive to the fraction mature and therefore to the way the threshold was represented

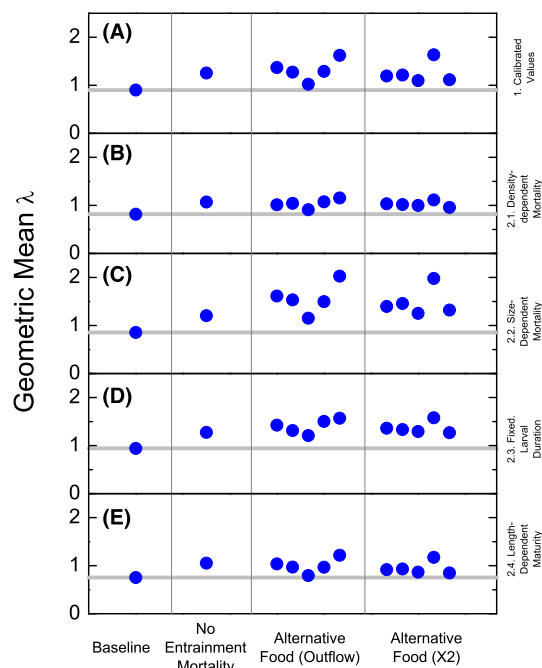


FIGURE 4. Geometric mean values of the annual finite population growth rate (λ) for Delta Smelt computed over the 10 years of each simulation for experiment 1 and the subsets of experiment 2, arranged as in Figure 3. Each dot corresponds to the geometric mean of the 10 values represented by each line in Figure 3; the horizontal lines show the respective baseline values. [Color figure can be viewed at afs.journals.org.]

through the young-of-the-year and adult stages. These results were similar in experiment 2, although differences in juvenile survival were apparent with density dependence (subset 2.1; Figure 5D). Additionally, in some years (e.g., 1998–2000), eliminating entrainment mortality allowed for higher larval survival and therefore more fish entering the juvenile stage, which lowered juvenile survival in the density-dependent experiment relative to the density-independent case.

Historical Food

The patterns of λ with historical zooplankton were more complex than those for eliminating entrainment mortality, mainly because of the imperfect matching of years and because not every year in the historical record had higher zooplankton biomass than its matched year in the model period (Figures 2 and 3F–O). In particular, feeding conditions in 1998 were apparently comparable to those in the historical period (Figure 3F, K). Nevertheless, in both experiments 1 and 2 (Figure 3F–O), λ values were generally higher with historical food than with present-day food, and these differences were greatest during the latter half of years in the model period.

Geometric mean λ values were similar among runs using historical zooplankton and mostly higher than corresponding values using present-day food whether years

were matched with outflow (third column in Figure 4) or with X2 (fourth column in Figure 4). The average of the five geometric means of λ in experiment 1 was 1.32 based on outflow and 1.25 based on X2—both about 40% higher than the baseline value of 0.90 (Table 5). Results of experiment 2 were qualitatively similar to those of experiment 1, with some quantitative differences. The food effect was somewhat dampened in experiment 2 subset 2.1 (density-dependent mortality), as higher juvenile abundance arising from better food conditions triggered a higher daily mortality rate (Figure 4B). The geometric mean λ for subset 2.1 increased by only about 25% with historical food compared to present-day food (geometric mean $\lambda = 1.04$ for matching with outflow and 1.03 for matching with X2; Table 5). The food effect was stronger in subset 2.2 (size-dependent mortality; Figure 4C) than in experiment 1. The geometric mean λ under this alternative baseline was 0.85 compared with the average of the five geometric means with historical food based on outflow (1.57) or on X2 (1.48), which equated to increases of approximately 80% (Table 5).

Survival through most life stages was insensitive to the substitution of historical food for present-day food (experiment 1; Figure 6). Survival of non-feeding yolk-sac larvae showed little effect of this substitution (Figure 6A). Unexpectedly, the survival of larvae was generally lower with historical food than with present-day food (Figure 6B). Survival of postlarvae was higher in most historical food sequences than with present-day food, especially after about 2001 (Figure 6C). Survival of juveniles and adults (age 1 to age 2) was not much affected by the substitution of historical for present-day food (Figure 6D, E).

In contrast to results for survival, mean length at recruitment (entering age 1) was considerably greater for historical food than for present-day food (experiment 1; Figure 7A). This resulted in much higher egg production (Figure 7C) because nearly twice as many recruits reached the length criterion for maturity by January 1 under historical food conditions (Figure 7B) and because individual fecundity increased exponentially with length (see equation 1 in Rose et al. 2013a). Faster growth may also have allowed for some repeat spawning. The higher egg production per recruit resulted in population abundance on January 1 of the final year that, under density independence, was about 10–100-fold higher than with present-day food (Figure 7D).

Recruits were larger with historical food than with present-day food because of faster growth, mainly during the juvenile life stage. The juvenile stage began when postlarvae reached a prescribed length but ended on January 1. Therefore, the average stage duration for juveniles was not a direct function of their growth rate. The P -values, which measure feeding success, were consistently higher for juveniles under historical food conditions determined

TABLE 4. Calculations of the major Delta Smelt model output variables and where displayed.

Variable	Model calculations	Display
Population growth rate (λ)	Eigenvalue analysis of the matrix model for each year of simulation	Figures 3, 4; Tables 5, 6
Population size	Summed worths of recruits (new age-1) and new age-2 super-individuals on January 1	Figure 7D
Annual recruitment	Summed worths of the new age-1 super-individuals on January 1	Used in Figure 7A–C
Mean length of recruits	Mean length of all new age-1 super-individuals on January 1, weighted by their worths	Figure 7A
Fraction of age-1 mature	Summed worths of age-1 fish larger than 60 mm at projected spawning divided by the summed worths of all age-1 fish	Figure 7B
Eggs per recruit	Total number of eggs produced by age-1 super-individuals in a year divided by recruitment on January 1 of that year	Figure 7C
Fraction surviving a stage	Summed worths of super-individuals exiting a life stage divided by the summed worths when they entered that stage	Figures 5, 6
Average stage duration	Number of days between dates of entry into and exit from each stage, averaged over super-individuals weighted by worths upon entry	Figure 9
Mean annual <i>P</i> -value by stage	Computed from daily population values of realized consumption expressed as a proportion of maximum consumption (<i>P</i> -value) for each box, averaged across boxes weighted by the proportion of individuals in each box. These values were then averaged over days for each year, weighted by the total population size on each day	Figure 8

by X2 than under present-day food conditions (Figure 8C); *P*-values were lower for larvae under historical food conditions than under present-day conditions (Figure 8A) and were generally similar between historical and present-day food for the other feeding stages (Figure 8B, D). Larvae grew more slowly with historical food than present-day food, thus extending the larval stage (Figure 9A). Average duration of the postlarval stage was slightly less—indicating faster growth—with historical food than present-day food (Figure 9B). Postlarvae fed at about the same rate under the different food conditions, except for slightly higher feeding rates under historical food conditions after 2001 (Figure 8B).

Age-1 adults grew from January 1 to their spawning dates at about the same rate irrespective of food conditions. From age 1 to age 2, adults gained a mean annual weight increment of 2.38–2.50 g with historical food, similar to that with present-day food (2.46 g).

Entrainment Mortality Compared with Historical Food

In experiments 1 and 2, eliminating entrainment mortality generated an increase in the geometric mean λ between 0.5 and 1.5 times the increase produced by substituting historical for present-day food (Table 5). In

experiment 1, eliminating entrainment mortality yielded a 39% increase in λ , which was identical to the average increase from substituting historical food for present-day food using X2 and lower than the average increase obtained from food substitution based on outflow (47%). The geometric mean λ was 0.90 under the baseline versus 1.25 with no entrainment mortality and present-day food; averaged 1.32 for the five outflow simulations of historical food; and averaged 1.25 for the five X2 simulations of historical food. Subset 2.1 (density-dependent mortality) had the smallest response to historical food ($\lambda \sim 26\%$ higher than that achieved under the baseline) and a similar increase with no entrainment mortality ($\lambda \sim 30\%$ higher than baseline). Subset 2.2 (size-dependent mortality) showed the largest response to the substitution of historical food for present-day food ($\lambda \sim 80\%$ higher than baseline), about twice the effect of eliminating entrainment mortality.

Experiment 2 subset 2.3 (fixed larval growth) showed that the results did not depend on the counterintuitive result of food being lower for larvae in historical than present-day conditions (see above). Eliminating entrainment mortality resulted in a λ value that was 35% higher than that generated under baseline conditions, while

TABLE 5. Geometric mean (GM) values of the annual finite population growth rate (λ) for Delta Smelt and the percent increase from the corresponding baseline λ for the zero entrainment mortality simulation and for historical food based on outflow or based on X2 (defined in Methods) from experiments 1 and 2 (experiment 2 subsets 2.1–2.4 are defined in Table 3).

Experiment	Baseline	No entrainment mortality		Historical food: outflow		Historical food: X2	
	GM	GM	Percent increase	Average of 5 GMs	Percent increase	Average of 5 GMs	Percent increase
1. Original (calibrated)	0.90	1.25	39	1.32	47	1.25	39
2.1. Density-dependent mortality	0.82	1.07	30	1.04	27	1.03	26
2.2. Size-dependent mortality	0.85	1.21	42	1.57	85	1.48	74
2.3. Fixed larval growth	0.94	1.27	35	1.40	49	1.37	46
2.4. Length-dependent maturity	0.75	1.05	40	1.00	33	0.95	27

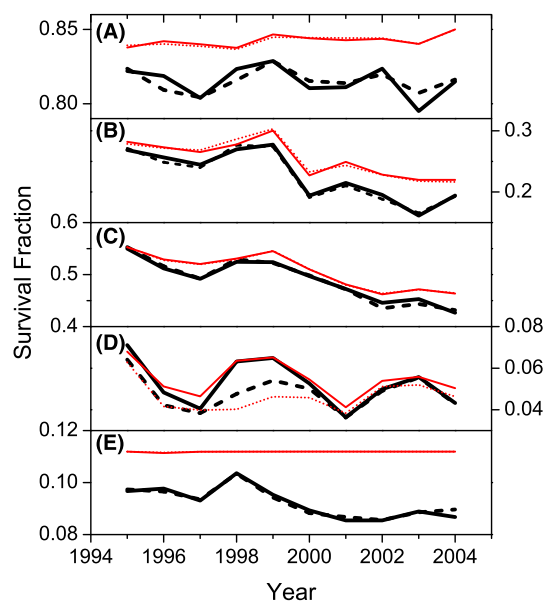


FIGURE 5. Model time series of the fraction of Delta Smelt that survived through each of five life stages for the experiment 1 (original) baseline (thick solid line) and zero entrainment mortality simulation (thin solid line); and for the experiment 2 subset 2.1 (density-dependent; see Table 3) baseline (thick dashed line) and zero entrainment mortality simulation (thin dotted line). Note the difference in scale among panels. Life stages are (A) yolk-sac larva, (B) larva, (C) postlarva, (D) juvenile, and (E) age-1 to age-2 adult. [Color figure can be viewed at afs.journals.org.]

substituting historical for present-day food resulted in a λ that was about 47% higher than baseline. Only in subset 2.4 (length-dependent maturity) did eliminating entrainment mortality cause a larger increase in λ (40% higher than baseline) than substituting historical food (33% increase for outflow and 27% increase for X2 relative to baseline).

The effects of eliminating entrainment mortality and using historical food were nearly independent (Table 7). For each of the historical food substitutions based on X2,

the geometric mean of the λ values when both entrainment mortality was eliminated and historical food was used (experiment 3) was very close to the products of the λ values obtained when the two factors were included in separate simulations (experiment 1). Moreover, the mean ratio of the two geometric mean λ values was very close to 1.0 (i.e., 1.03; Table 7) across all five X2 simulations.

DISCUSSION

Our model for Delta Smelt capitalizes on the availability of valuable long-term monitoring data, which include multiple sampling events for fish and their environment throughout the Delta Smelt life cycle. The model uses fine-scale output from a hydrodynamic model to investigate how spatially and temporally specific factors may have affected Delta Smelt population dynamics. Both historical changes in zooplankton and entrainment losses can affect Delta Smelt on fine temporal and spatial scales. These two factors were selected for detailed investigation because of management interest (described above) and because previous modeling had shown that development to maturity (related to feeding) and hydrodynamic conditions (controlling entrainment) were important factors distinguishing the years with the highest and lowest population growth rates of Delta Smelt (Rose et al. 2013b). Other potentially important factors not included in the model are discussed below.

Entrainment Effects

Eliminating mortality due to entrainment increased the geometric mean λ by 39% in experiment 1 (Table 5). This increase was due to higher survival of adult and larval life stages. Note that adult mortality was calibrated to match estimates averaged over the model period, while larval mortality depended only on their transport with the water. Thus, our analysis of effects on adults over all model years is a consequence of the calibration, while effects on larvae were an uncalibrated outcome of the simulated

TABLE 6. Daily mortality values for Delta Smelt by life stage, including parameters used as inputs to the model and means for the experiment 1 baseline and zero entrainment mortality simulation during 1996–2000 and 2001–2005; and survival proportions over the mean duration of the young-of-the-year and adult stages (survival through stage = e^{-mD} , where D is 239 d for young of the year and 365 d for adults).

Year-class	Stage	Mortality parameter	1996–2000		2001–2005	
			Baseline	No entrainment mortality	Baseline	No entrainment mortality
Young of the year	Yolk-sac larva	0.035	0.040	0.036	0.043	0.035
	First-feeding larva	0.050	0.054	0.052	0.058	0.053
	Postlarva	0.030	0.031	0.031	0.034	0.030
	Juvenile	0.015	0.016	0.015	0.016	0.015
	Total ^a	0.021	0.0232	0.0227	0.0264	0.0251
Age-1 adult	Age-1 adult	0.006	0.0064	0.0061	0.0067	0.0060
Survival through Stage						
Young of the year	Young of the year	0.0072	0.0039	0.0043	0.0018	0.0025
Age-1 adult	Age-1 adult	0.112	0.097	0.112	0.087	0.112

^aThe total young-of-the-year mortality shown here is not a parameter in the model. The values in this row of the table were calculated from the input mortality values by stage and the mean durations of each stage estimated from the model output. The year 1995 was omitted because entrainment effects carried over from the four spin-up years of the model runs.

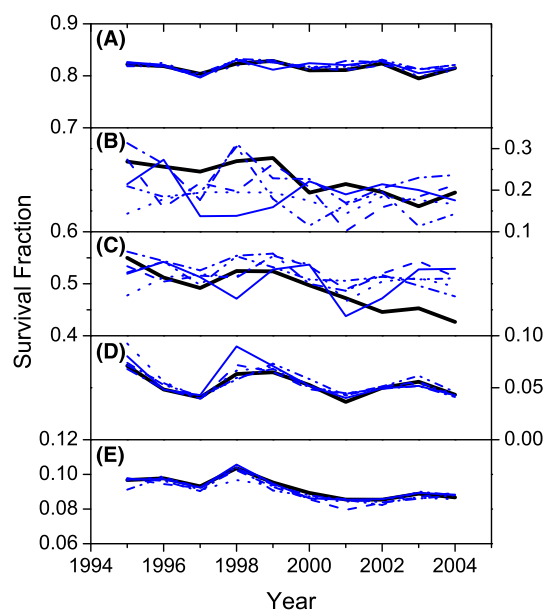


FIGURE 6. Same as in Figure 5 for the experiment 1 original baseline (thick line) and the five historical food simulations based on X2 (thin lines; X2 is defined in Methods) for each life stage of Delta Smelt: (A) yolk-sac larva, (B) larva, (C) postlarva, (D) juvenile, and (E) age-1 to age-2 adult. [Color figure can be viewed at afsjournals.org.]

movements of water and particles in the model. Mean survival was 21% higher for adults and 22% higher across all subadult stages with entrainment mortality eliminated than under the original baseline (Table 6; Figure 5). The difference in survival of young-of-the-year individuals between baseline and the simulation with no entrainment mortality decreased with stage as the model fish moved

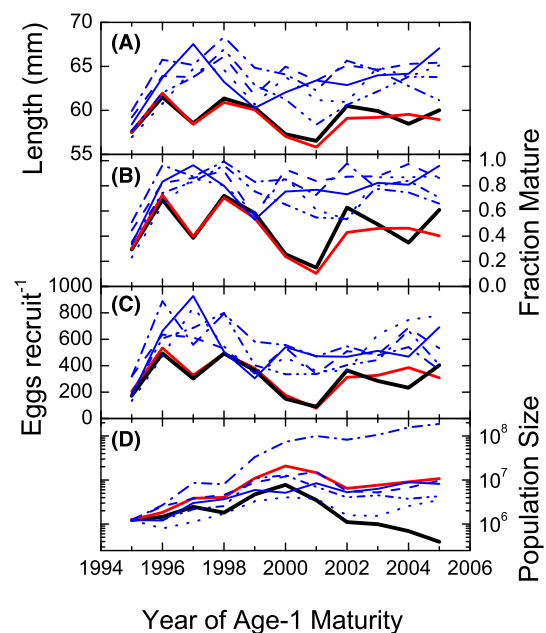


FIGURE 7. Model time series of key population metrics for Delta Smelt in experiment 1: (A) mean length of recruits; (B) fraction of recruits that were mature; (C) number of eggs per recruit; and (D) population size on January 1. The thick line represents the original baseline; the medium line represents the zero entrainment mortality simulation; and the thin lines represent historical food simulations based on X2 (defined in Methods). [Color figure can be viewed at afsjournals.org.]

from freshwater to brackish water, where they are less vulnerable to entrainment. In dry years, when larvae and adults are farther up-estuary and therefore more vulnerable to entrainment, the proportional difference in survival

TABLE 7. Geometric mean annual finite population growth rate (λ) for Delta Smelt in experiment 3 (zero entrainment mortality and historical food combined) and the product of the geometric mean λ values for simulations with zero entrainment mortality only and for simulations with historical food from experiment 1 based on the five substitute years matched for X2 (defined in Methods; year substitutions are specified in Table 2).

Year substitution	(A) Experiment 3: zero entrainment mortality and historical food combined	(B) Experiment 1: zero entrainment mortality \times historical food	Ratio of A:B
1	1.97	$1.40 \times 1.33 = 1.85$	1.07
2	1.89	$1.40 \times 1.35 = 1.89$	1.00
3	1.79	$1.40 \times 1.22 = 1.70$	1.05
4	2.69	$1.40 \times 1.81 = 2.53$	1.06
5	1.69	$1.40 \times 1.24 = 1.72$	0.98
Mean			1.03

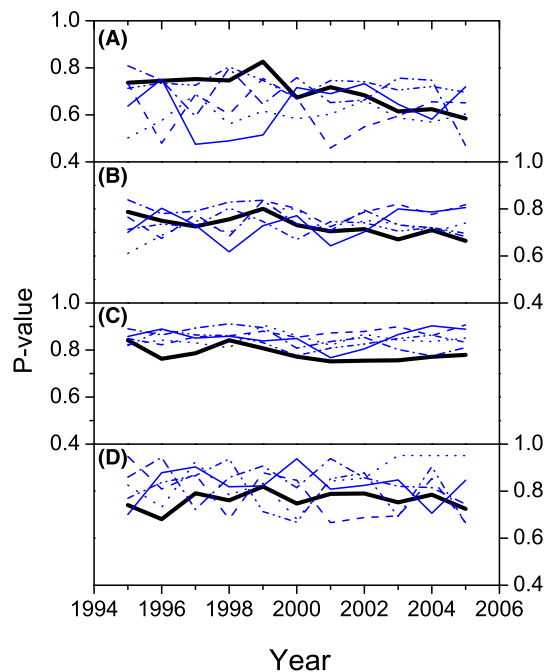


FIGURE 8. Annual mean values of the ratio of realized consumption to maximum consumption (P -value) for the experiment 1 original baseline (thick line) and historical food simulations based on X2 (thin lines; X2 is defined in Methods) for Delta Smelt life stages: (A) larva, (B) postlarva, (C) juvenile, and (D) age-1 to age-2 adult. [Color figure can be viewed at afsjournals.org.]

between baseline and zero entrainment mortality scenarios was as high as 48% for early life stages (32% not counting juveniles) and 31% for adults (e.g., Figure 5A, B, E for 2001).

Effects of uncertainty in entrainment mortality were of similar magnitude to effects of the alternative baseline assumptions (Table 5). Kimmerer's (2008, 2011) analysis of adult entrainment mortality used monitoring data to estimate a parameter Θ that was proportional to mean

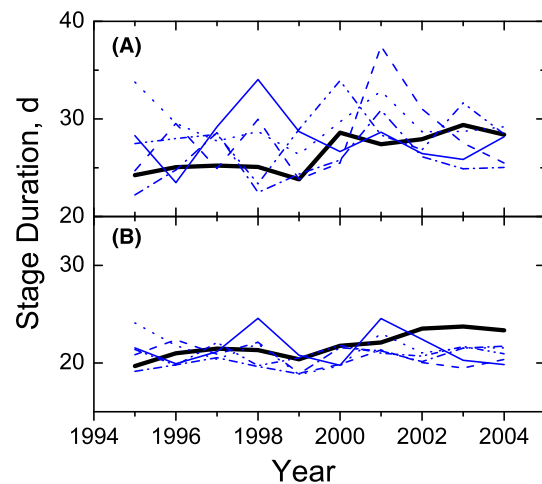


FIGURE 9. Model time series of average stage durations (d) of Delta Smelt (A) larvae and (B) postlarvae for the experiment 1 original baseline and historical food simulations based on X2 (defined in Methods). [Color figure can be viewed at afsjournals.org.]

entrainment mortality; the resulting 95% credible interval of Θ was -40% to $+50\%$ of its mean value. Because adult entrainment mortality in our model was calibrated to the mean entrainment mortality calculated by Kimmerer (2008, 2011) and because entrainment losses of adults in the model are about half of the simulated total entrainment losses (see above), uncertainty in the modeled value of total entrainment mortality is roughly half of that for Θ above. Although additional IBM simulations can be done, we simply assumed percent changes in age-1 and age-2 annual survival fractions and recomputed λ from the adjusted matrix projection model (see Appendix in Rose et al. 2013b). In general, the uncertainty in annual entrainment survival (represented by changes in age-specific survival fractions) translated to similar or smaller

changes in λ depending on the matrix model realized for each year. For example, assuming high uncertainty in annual adult entrainment ($\pm 50\%$ in age-1 and age-2 survival fractions, which also affect the fecundity-related elements of the matrix) resulted in about $\pm 50\%$ changes in λ . Thus, the uncertainty inferred for the added daily mortality term based on Old and Middle River flow would affect λ similarly to the use of alternative baselines ($\sim 25\text{--}74\%$ changes in average λ ; Table 5) that reflect structural uncertainties in the model. In addition, our comparisons focused on contrasting entrainment with zero entrainment; such an extreme contrast (compared with the effects of small changes in entrainment) lends robustness to our results. None of these sources of uncertainty contradicts the conclusion that in some years, entrainment mortality is an important constraint on the population growth of Delta Smelt.

Our analyses eliminated entrainment mortality without changing flow patterns. A fuller exploration of these effects would require (1) determination of an alternative hydrology to reflect operational controls for achieving the reduced entrainment and (2) modeling of the responses of fish to the new, altered hydrodynamic conditions. Such an effort would require substantial modeling work by management agencies and was well beyond the scope of our project.

Food Effects

The increases in modeled population growth rate from substituting historical food for model period food bracketed the increase from eliminating entrainment mortality in experiment 1 (Table 5), but these responses occurred through different mechanisms. Eliminating entrainment mortality increased survival. In contrast, historical food supported higher rates of consumption by most life stages (Figure 8) and faster growth of juveniles, leading to larger recruits and a higher proportion of recruits that were mature on January 1, which together caused higher egg production per recruit (Figure 7). Similarly, the major difference between the best and worst years in the baseline run was due to the effect of juvenile growth on the proportion of Delta Smelt that were mature by the spawning period and on their subsequent age-1 egg production (Rose et al. 2013b).

Outcomes varied among the various historical food substitute years (Table 2) because of interannual differences in hydrology and in spatial and temporal patterns of zooplankton abundance, as shown in the example (Figure 2). Obvious differences between the model and historical periods included the absence of two species in the historical years (Figure 2A, F) and the higher biomass of the other taxa in most historical years (Figure 2B–E). For example, the former key prey species *Eurytemora affinis* (Figure 2E) was nearly absent during the model period

years (Winder and Jassby 2011). Much of the variability in zooplankton biomass among substitute years was a result of spatial differences, and the model spatial boxes other than that presented in the example (Figure 2) show somewhat different biomass patterns among individual years.

Larvae had a different response to the substitution of historical food than did the other life stages in the model. Counterintuitively, *P*-values for larvae were generally lower with historical food than under baseline conditions (Figure 8A). In the model, larvae consumed only juvenile calanoid copepods and adults of the cyclopoid *L. tetraspina*; the other four zooplankton groups were considered too large to be available to larvae based on laboratory observations (Sullivan et al. 2016). In addition, we had specified low feeding efficiency of larval Delta Smelt on adults of *L. tetraspina*. Recent diet analysis indicates that during April 2005 and 2006, larval Delta Smelt obtained most of their food biomass from copepodites and ate very low quantities of *L. tetraspina* (Slater and Baxter 2014). Calanoid copepodites were more abundant in some model period years than in historical years because between these periods several copepod species were introduced to the SFE, including *P. forbesi*, which had variable overlap with Delta Smelt in the low-salinity habitat (Kimmerer et al. 2017).

Several taxa, including copepod nauplii, cyclopoid copepodites, and cladocerans, made up at least 1% of the mass of Delta Smelt gut contents in spring 2005–2006 (Slater and Baxter 2014). These taxa were not included in the model, but all were more abundant before 1987 (when an invasive clam caused massive changes in the food web; Alpine and Cloern 1992; Kimmerer et al. 1994) than during the model period. Thus, the low feeding success of larvae with historical food may indicate that our representation of Delta Smelt food based on the model period was incomplete. Modeled effects of entrainment and historical food on λ of Delta Smelt were nevertheless robust to the reduced growth of larvae under historical food, as results were similar when larval growth rate was fixed in simulations (subset 2.3; Table 3).

Alternative Baseline Formulations (Experiment 2)

Evidence for density dependence is apparent in the data for Delta Smelt during periods of high juvenile abundance in summer and subsequent moderate autumn abundance in the 1970s (Bennett 2005). However, after the declines of Delta Smelt in the 1980s, evidence for density dependence has been weaker and suggests a lower carrying capacity (Bennett 2005). The mechanism for this saturating form of density dependence may be related to habitat availability or food limitation (Bennett 2005) or possibly to prey switching by piscivores such as Striped Bass *Morone saxatilis* (Nobriga et al. 2013).

Others have used the long-term monitoring data to infer density-dependent mortality in Delta Smelt. Maunder and Deriso (2011) fitted a state-space model with several covariates to abundance indices of Delta Smelt from 1972 to 2006 and found evidence for a Ricker-type density-dependent mortality (i.e., survival decreasing across the range of juvenile abundance) between summer and fall and weaker, saturating density dependence between fall and spring. Likewise, Miller et al. (2012) imposed a Ricker-type density-dependence relationship on survival in their models. However, it is difficult to reconcile this form of survival with an annual pelagic fish at historically low abundance. Moreover, no mechanism for such density-dependent mortality has been proposed. If density-dependent mortality occurs, it is likely to be a local phenomenon (Walters and Korman 1999). Such local interactions are amenable to modeling with a spatially explicit IBM, as we have done in experiment 2, in which juvenile mortality rate increased with the degree of local crowding (see equation 2 in Rose et al. 2013b).

Including density-dependent mortality in the juvenile stage (subset 2.1; Table 3) dampened variability relative to the results of experiment 1 (Figure 4B) in the geometric mean λ among the historical food matchings and reduced the magnitude of the effects of eliminating entrainment mortality and increasing the food supply. However, the relative magnitudes of effects between the zero entrainment mortality and historical food simulations remained similar to those from experiment 1 (Figure 4; Table 5).

The alternative baseline with size-dependent mortality instead of stage-dependent constant mortality (subset 2.2) represented mortality as a power function of length, with the mortality rates matched to the stage-dependent case at the midpoints of each stage (see equation 1 in Rose et al. 2013b). This resulted in little change in the effect of eliminating mortality and an amplification of the food effect relative to that in experiment 1 (Table 5). This amplification was due to higher juvenile survival with size-dependent mortality than with stage-dependent mortality (results not shown). Because super-individuals that grew faster survived better through the juvenile stage, this alternative size-dependent mortality enhanced the effect of food on size and survival of the maturing fish. This enhancement of survival with plentiful food is suggested by a positive relationship between zooplankton biomass and the ratio of fall to summer abundance indices (Kimmerer 2008).

The alternative baseline that substituted a fixed growth rate for the bioenergetics and feeding functions of larvae (subset 2.3) was selected because of uncertainty in larval bioenergetics parameters and uncertainty about the foods that were actually consumed by larvae during the historical period. In experiment 1, the effect of historical food was negative (i.e., food was less available to the larval

stage), and as discussed above, this is likely an artifact of incomplete knowledge of larval feeding and of the prey field. The positive effect of historical food on the geometric mean λ in subset 2.3 was somewhat larger than that in experiment 1 because the effect of low historical food biomass during the larval stage no longer played a role. Additional information on larval bioenergetics and prey consumption would help to refine the model and increase confidence when the model is used to investigate other food-related questions involving Delta Smelt larvae.

The original baseline had a length threshold for maturity, and the proportion of recruits that were mature strongly influenced the effect of historical food on population growth. We therefore included an alternative function for maturity (subset 2.4) that used a smooth dependence of maturity on length instead of a threshold length (Table 3). This was the only subset of experiment 2 for which the effect of eliminating entrainment mortality was clearly larger than the effect of historical food (Table 5). As with the other alternative functions in experiment 2, this modification of the model affected the comparison of entrainment and historical food effects quantitatively but not qualitatively.

What is Not in the Model?

Several potentially important aspects of Delta Smelt ecology have been simplified or omitted from the model. This was done because of our focus on comparing the relative effects of entrainment versus food web changes but also because information available for the model period was inadequate to parameterize some of these other influences on the Delta Smelt population. If this model is used for additional analysis, these aspects should be revisited.

Predation was represented as a stage-specific mortality rate, and temporal and spatial effects of predators were not explicitly represented. Variation in predation is probably an important driver of within-year and interannual changes in Delta Smelt abundance (Ferrari et al. 2013; Nobriga et al. 2013) and may also influence Delta Smelt indirectly by restricting where and when they can feed (Walters and Korman 1999; Railsback and Harvey 2011). However, information is lacking on fine-scale population densities and feeding rates of likely predators of Delta Smelt (Nobriga et al. 2013). For example, Mississippi Silversides *Menidia beryllina* prey upon Delta Smelt larvae (Schreier et al. 2016) and have increased greatly in abundance in shallow waters (Bennett 2005), but they are not quantitatively sampled by any monitoring program. The most likely predators on juvenile and adult Delta Smelt are Striped Bass (Nobriga et al. 2013) and Largemouth Bass *Micropterus salmoides*. Largemouth Bass have increased in abundance with the expansion of waterweeds in the Delta (Brown and Michniuk 2007; Ferrari et al.

2013; Conrad et al. 2016), but population consumption rates of Delta Smelt are not available for either of these predators.

Turbidity also was not included in the model, although it explained 21% (in summer) or 13% (in autumn) of the deviance in log catch per trawl in two long-term surveys (Feyrer et al. 2007, 2011; Nobriga et al. 2008). Young Delta Smelt that are held in clear water show evidence of physiological stress and will not feed readily, suggesting that low turbidity may limit larval feeding success in the estuary (Baskerville-Bridges et al. 2004; Hasenbein et al. 2013, 2016). Lower abundance of Delta Smelt in clear water than in turbid water may occur because they avoid clear water or are eaten by predators in clear water (Feyrer et al. 2007, 2011; Nobriga et al. 2008). In addition, capture of adult Delta Smelt at the fish extraction facilities associated with the water diversions is weakly but positively related to turbidity (Grimaldo et al. 2009) and has been used in managing diversion flows. Thus, omitting this factor may have caused us to overestimate entrainment losses in recent modeled years owing to a possible decline in turbidity.

We excluded turbidity from the IBM for several reasons. First, continuous monitoring for turbidity in the Delta began only in 2000, and the records of turbidity from shipboard sampling are too sparse in space and time to permit modeling of this highly variable property. Second, turbidity could have played a role in modeled juvenile and adult Delta Smelt movement, but we determined that it was not needed. We opted to use only salinity as the movement cue because salinity is consistently correlated with Delta Smelt spatial distributions (Feyrer et al. 2007; Nobriga et al. 2008; Rose et al. 2013a) and varies on monthly and regional (model box) scales that were the target of our simulated movement. Turbidity varies at spatial scales finer than that of our spatial boxes and is also episodic (Fichot et al. 2016), which complicates the simulation of Delta Smelt movement on seasonal and regional scales. Third, our main purpose was to explore the effects of entrainment and food supply; although these are likely linked to turbidity, the quantitative nature of that link is unclear, and each of the proposed mechanisms for turbidity effects would require a different model formulation and would not be amenable to testing with the model because of the lack of data. Fourth, turbidity in the SFE has decreased over several decades (Kimmerer 2004), so forcing a turbidity effect into the model in the absence of a clearly supported mechanism would produce an apparent but potentially misleading covariation with declining Delta Smelt abundance. Our model predicted the decline in Delta Smelt over the 1995–2005 model period without imposing a monotonically changing driving variable (Rose et al. 2013a).

Likewise, we lacked a basis for modeling contaminant effects on Delta Smelt, although they are likely to be

important at some times and places. Effects of ammonium and other contaminants on Delta Smelt have been documented in bioassays (Hasenbein et al. 2014) and histopathologic studies (Hammock et al. 2015). However, contaminant effects too are highly localized, and available data were insufficient to provide a description of the spatial and temporal pattern of these effects.

All Delta Smelt individuals in our model were created equal; no allowance was made for variability in their life history traits and strategies outside of stochastic variation in movement. Like many estuarine fish species (Secor 1999), Delta Smelt may express more than one life history strategy. A contingent of Delta Smelt remains year-round in a freshwater region of the northern Delta despite high temperature, low salinity, and chronic toxicity (Sommer et al. 2011; Hammock et al. 2015). Furthermore, some Delta Smelt will spawn in rivers west of Suisun Bay (Figure 1) during times of high freshwater runoff (Hobbs et al. 2006). To include these characteristics in the IBM would require expanding the hydrodynamic model grid to the west and would require a better mechanistic understanding of the cues triggering these alternative life histories and spawning migration patterns.

Delta Smelt feed heavily on copepods during early life (Nobriga 2002; Feyrer et al. 2003). The taxa included among the six groups of copepods in the model comprised 89% (median by year and month; range = 32–99%) of the biomass of food taxa reported for larval to juvenile Delta Smelt during April–September 2005 and 2006 (Slater and Baxter 2014). Delta Smelt consumed small amounts of amphipods and mysids during summer (0–9% of the mass of gut contents during July–September; Slater and Baxter 2014) and likely consume more of these larger prey types as they reach adulthood, particularly because calanoid copepods are uncommon in winter (Kimmerer and Orsi 1996). Thus, the model's representation of feeding by both first-feeding larvae and adults should be improved as new information on feeding and growth becomes available.

Potential Remedial Actions

Clearly, both entrainment and changes in the zooplankton food base are important for the annual survival and population growth of Delta Smelt and present challenges for remedial and management actions. Reducing entrainment mortality, although easy in the virtual world, can be impracticable or costly in the real world. High precipitation in northern California and high demand for water in southern California necessitate the transfer of water from north to south. Although several alternative approaches to this practice have been suggested (Lund et al. 2007), the remedial actions for entrainment losses with the current system of statewide water use are limited to reducing diversion flow, increasing freshwater flow through the Delta, and moving the point of diversion upstream of

Delta Smelt habitat. Although increasing freshwater outflow may seem like a viable management tool for reducing entrainment of Delta Smelt, the financial cost of using stored water to achieve meaningful increases in outflow during dry periods is very high (Kimmerer 2002), and water is in shortest supply during dry winters and springs when the Delta Smelt are most vulnerable to entrainment (Kimmerer 2008). The state of California is planning to construct a facility to divert water from the Sacramento River around the Delta to the south Delta diversion facilities at a cost of approximately US\$15 billion (<http://www.californiawaterfix.com>). The Delta Smelt IBM could be used to analyze the effectiveness of the altered diversion scheme for protecting Delta Smelt if the predicted flows and zooplankton dynamics become available on sufficiently detailed temporal and spatial scales.

Two other possibilities have been suggested for improving conditions for the Delta Smelt and other fishes. The first is an expansion of physical habitat by restoring former wetlands to tidal action. Although the Delta Smelt is a pelagic fish, the apparent ability of some Delta Smelt to remain in tidal lakes in the northern Delta through summer (Merz et al. 2011; Sommer and Mejia 2013) suggests that enlarging this habitat might provide a greater choice of alternative rearing sites. This suggestion could be modeled with the IBM by setting movement rules to allow some fish to remain in the northern Delta. Another suggested action is to restore shallow tidal areas to export excess zooplankton to the open waters of the estuary. Although conceptually this action would address a key impediment to the recovery of Delta Smelt, it lacks a solid scientific basis (see Chapter 7 in Mount et al. 2014). Recently, the scope of this plan has been scaled back, and it is no longer aimed principally at Delta Smelt (http://resources.ca.gov/docs/ecorestore/ECO_FS_Overview.pdf).

The Long-term Trend in Delta Smelt Abundance

Since the decline in abundance of four fish species of the upper SFE during the early 2000s (Sommer et al. 2007), Delta Smelt abundance indices have continued a general downward trend, except for brief rebounds during high-flow years such as 2011 (IEP-MAST 2015). Nevertheless, several indices reached record lows in 2015. The causes of those declines have remained uncertain and controversial (Baxter et al. 2010; Mac Nally et al. 2010; Thomson et al. 2010). A recent synthesis concluded that the high abundance in 2011 likely resulted from reduced entrainment and higher food availability as well as lower temperature and lower abundance of the toxic cyanobacterium *Microcystis aeruginosa* (IEP-MAST 2015).

Our results support the conclusion (IEP-MAST 2015) that reduced entrainment and elevated zooplankton

densities would contribute at ecologically meaningful levels to the recovery of Delta Smelt. Integrating population modeling into the data analysis and adaptive management efforts would leverage the ongoing efforts for comparing the likely causes of the decline and for developing ecologically based, cost-effective remedial actions. More generally, population modeling could be used to guide policymakers in applying current scientific knowledge to their decisions.

ACKNOWLEDGMENTS

We thank K. P. Edwards and W. A. Bennett for work to develop and provide inputs to the IBM. K. B. Newman provided helpful advice throughout our investigations, and comments by M. J. Weaver, J. A. Hobbs, and anonymous reviewers improved the manuscript. Funding for model development was provided by the CALFED Science Program (now Delta Science Program; SCI-05-C106). Funding for analysis was provided by Cooperative Agreement Number R12AC20014 between the U.S. Bureau of Reclamation and San Francisco State University.

REFERENCES

- Alpine, A. E., and J. E. Cloern. 1992. Trophic interactions and direct physical effects control phytoplankton biomass and production in an estuary. *Limnology and Oceanography* 37:946–955.
- Baskerville-Bridges, B., J. C. Lindberg, and S. I. Doroshov. 2004. The effect of light intensity, alga concentration, and prey density on the feeding behavior of Delta Smelt larvae. Pages 219–227 in F. Feyrer, L. R. Brown, R. L. Brown, and J. J. Orsi, editors. *Early life history of fishes in the San Francisco Estuary and watershed*. American Fisheries Society, Bethesda, Maryland.
- Baxter, R., R. Breuer, L. Brown, L. Conrad, F. Feyrer, S. Fong, K. Gehrts, L. Grimaldo, B. Herbold, P. Hrodey, A. Mueller-Solger, T. Sommer, and K. Souza. 2010. 2010 Pelagic Organism Decline Work Plan and synthesis of results. Interagency Ecological Program for the San Francisco Estuary, Sacramento, California.
- Bennett, W. A. 2005. Critical assessment of the Delta Smelt population in the San Francisco Estuary, California. *San Francisco Estuary and Watershed Science* [online serial] 3(2):1.
- Bennett, W. A., and J. R. Burau. 2014. Riders on the storm: selective tidal movements facilitate the spawning migration of threatened Delta Smelt in the San Francisco Estuary. *Estuaries and Coasts* 38:826–835.
- Brown, L. R., W. Kimmerer, and R. Brown. 2008. Managing water to protect fish: a review of California's Environmental Water Account. *Environmental Management* 43:357–368.
- Brown, L. R., and D. Michniuk. 2007. Littoral fish assemblages of the alien-dominated Sacramento–San Joaquin Delta, California, 1980–1983 and 2001–2003. *Estuaries and Coasts* 30:186–200.
- Bryant, M. E., and J. D. Arnold. 2007. Diets of age-0 Striped Bass in the San Francisco Estuary, 1973–2002. *California Fish and Game* 93:1–22.
- Castillo, G., J. Morinaka, J. Lindberg, R. Fujimura, B. Baskerville-Bridges, J. Hobbs, G. Tigan, and L. Ellison. 2012. Pre-screen loss and fish facility efficiency for Delta Smelt at the south Delta's State Water Project, California. *San Francisco Estuary and Watershed Science* [online serial] 10(4):4.

- Cloern, J. E., and A. Jassby. 2012. Drivers of change in estuarine-coastal ecosystems: discoveries from four decades of study in San Francisco Bay. *Reviews in Geophysics* 50:1–33.
- Conrad, J. L., A. J. Bibian, K. L. Weinersmith, D. De Carion, M. J. Young, P. Crain, E. L. Hestir, M. J. Santos, and A. Sih. 2016. Novel species interactions in a highly modified estuary: association of Largemouth Bass with Brazilian waterweed *Egeria densa*. *Transactions of the American Fisheries Society* 145:249–263.
- Draper, A., A. Munevar, S. Arora, E. Reyes, N. Parker, F. Chung, and L. Peterson. 2004. CalSim: generalized model for reservoir system analysis. *Journal of Water Resources Planning and Management* 130:480–489.
- Ferrari, M. O., L. Ranaker, K. L. Weinersmith, M. Young, A. Sih, and J. L. Conrad. 2013. Effects of turbidity and an invasive waterweed on predation by introduced Largemouth Bass. *Environmental Biology of Fishes* 97:79–90.
- Feyrer, F., B. Herbold, S. A. Matern, and P. B. Moyle. 2003. Dietary shifts in a stressed fish assemblage: consequences of a bivalve invasion in the San Francisco Estuary. *Environmental Biology of Fishes* 67:277–288.
- Feyrer, F., K. Newman, M. Nobriga, and T. Sommer. 2011. Modeling the effects of future outflow on the abiotic habitat of an imperiled estuarine fish. *Estuaries and Coasts* 34:120–128.
- Feyrer, F., M. L. Nobriga, and T. R. Sommer. 2007. Multi-decadal trends for three declining fish species: habitat patterns and mechanisms in the San Francisco Estuary, California, U.S.A. *Canadian Journal of Fisheries and Aquatic Sciences* 64:723–734.
- Fichot, C. G., B. D. Downing, B. A. Bergamaschi, L. Windham-Myers, M. Marvin-DiPasquale, D. R. Thompson, and M. M. Gierach. 2016. High-resolution remote sensing of water quality in the San Francisco Bay Delta Estuary. *Environmental Science and Technology* 50:573–583.
- Grimaldo, L. F., T. Sommer, N. V. Ark, G. Jones, E. Holland, P. B. Moyle, B. Herbold, and P. Smith. 2009. Factors affecting fish entrainment into massive water diversions in a tidal freshwater estuary: can fish losses be managed? *North American Journal of Fisheries Management* 29:1253–1270.
- Gunderson, A. R., and M. Leal. 2016. A conceptual framework for understanding thermal constraints on ectotherm activity with implications for predicting responses to global change. *Ecology Letters* 19:111–120.
- Hammock, B. G., J. A. Hobbs, S. B. Slater, S. Acuna, and S. J. Teh. 2015. Contaminant and food limitation stress in an endangered estuarine fish. *Science of the Total Environment* 532:316–326.
- Hanak, E., J. Lund, A. Dinar, B. Gray, R. Howitt, J. Mount, P. Moyle, and B. Thompson. 2008. *Managing California's water: from conflict to reconciliation*. Public Policy Institute of California, San Francisco.
- Hanson, P. C., T. B. Johnson, D. E. Schindler, and J. F. Kitchell. 1997. *Fish Bioenergetics 3.0*. University of Wisconsin Sea Grant Institute, Madison.
- Hasenbein, M., N. A. Fanguie, J. Geist, L. M. Komoroske, J. Truong, R. McPherson, and R. E. Connon. 2016. Assessments at multiple levels of biological organization allow for an integrative determination of physiological tolerances to turbidity in an endangered fish species. *Conservation Physiology* [online serial] 4:cow004.
- Hasenbein, M., L. M. Komoroske, R. E. Connon, J. Geist, and N. A. Fanguie. 2013. Turbidity and salinity affect feeding performance and physiological stress in the endangered Delta Smelt. *Integrative and Comparative Biology* 53:620–634.
- Hasenbein, M., I. Werner, L. A. Deanovic, J. Geist, E. B. Fritsch, A. Javidmehr, C. Foe, N. A. Fanguie, and R. E. Connon. 2014. Transcriptomic profiling permits the identification of pollutant sources and effects in ambient water samples. *Science of the Total Environment* 468:688–698.
- Hobbs, J. A., W. A. Bennett, and J. E. Burton. 2006. Assessing nursery habitat quality for native smelts (Osmeridae) in the low-salinity zone of the San Francisco Estuary. *Journal of Fish Biology* 69:907–922.
- Humston, R., D. B. Olson, and J. S. Ault. 2004. Behavioral assumptions in models of fish movement and their influence on population dynamics. *Transactions of the American Fisheries Society* 133:1304–1328.
- IEP-MAST (Interagency Ecological Program, Management, Analysis, and Synthesis Team). 2015. An updated conceptual model of Delta Smelt biology: our evolving understanding of an estuarine fish. IEP, Technical Report 90, Sacramento, California.
- Jassby, A. D., J. E. Cloern, and B. E. Cole. 2002. Annual primary production: patterns and mechanisms of change in a nutrient-rich tidal estuary. *Limnology and Oceanography* 47:698–712.
- Jassby, A. D., W. J. Kimmerer, S. G. Monismith, C. Armor, J. E. Cloern, T. M. Powell, J. R. Schubel, and T. J. Vendlinski. 1995. Isohaline position as a habitat indicator for estuarine populations. *Ecological Applications* 5:272–289.
- Kimmerer, W. J. 2002. Physical, biological, and management responses to variable freshwater flow into the San Francisco Estuary. *Estuaries* 25:1275–1290.
- Kimmerer, W. J. 2004. Open water processes of the San Francisco Estuary: from physical forcing to biological responses. *San Francisco Estuary and Watershed Science* [online serial] 2(1):1.
- Kimmerer, W. J. 2008. Losses of Sacramento River Chinook Salmon and Delta Smelt to entrainment in water diversions in the Sacramento-San Joaquin Delta. *San Francisco Estuary and Watershed Science* [online serial] 6(2):2.
- Kimmerer, W. J. 2011. Modeling Delta Smelt losses at the south Delta export facilities. *San Francisco Estuary and Watershed Science* [online serial] 9(1):2.
- Kimmerer, W. J., J. R. Burau, and W. A. Bennett. 1998. Tidally-oriented vertical migration and position maintenance of zooplankton in a temperate estuary. *Limnology and Oceanography* 43:1697–1709.
- Kimmerer, W. J., E. Gartside, and J. J. Orsi. 1994. Predation by an introduced clam as the probable cause of substantial declines in zooplankton in San Francisco Bay. *Marine Ecology Progress Series* 113:81–93.
- Kimmerer, W. J., T. R. Ignoffo, K. R. Kayfetz, and A. M. Slaughter. 2017. Effects of freshwater flow and phytoplankton biomass on growth, reproduction, and spatial subsidies of the estuarine copepod *Pseudodiaptomus forbesi*. *Hydrobiologia* 807:113–130.
- Kimmerer, W. J., and M. N. Nobriga. 2008. Investigating particle transport and fate in the Sacramento-San Joaquin Delta using a particle tracking model. *San Francisco Estuary and Watershed Science* [online serial] 6(1):4.
- Kimmerer, W. J., and J. J. Orsi. 1996. Causes of long-term declines in zooplankton in the San Francisco Bay Estuary since 1987. Pages 403–424 in J. T. Hollibaugh, editor. *San Francisco Bay: the ecosystem*. American Association for the Advancement of Science, San Francisco.
- Lantry, B. F., and D. J. Stewart. 1993. Ecological energetics of Rainbow Smelt in the Laurentian Great Lakes: an interlake comparison. *Transactions of the American Fisheries Association* 122:951–976.
- Lindberg, J. C., G. Tigan, L. Ellison, T. Rettinghouse, M. M. Nagel, and K. M. Fisch. 2013. Aquaculture methods for a genetically managed population of endangered Delta Smelt. *North American Journal of Aquaculture* 75:186–196.
- Lund, J., E. Hanak, W. Fleenor, R. Howitt, J. Mount, and P. Moyle. 2007. *Envisioning futures for the Sacramento-San Joaquin Delta*. Public Policy Institute of California, San Francisco.
- Mac Nally, R., J. Thomson, W. Kimmerer, F. Feyrer, K. Newman, A. Sih, W. Bennett, L. Brown, E. Fleishman, S. Culberson, and G. Castillo. 2010. An analysis of pelagic species decline in the upper San Francisco Estuary using multivariate autoregressive modelling (MAR). *Ecological Applications* 20:1417–1430.

- Maunder, M. N., and R. B. Deriso. 2011. A state-space multistage life cycle model to evaluate population impacts in the presence of density dependence: illustrated with application to Delta Smelt (*Hypomesus transpacificus*). *Canadian Journal of Fisheries and Aquatic Sciences* 68:1285–1306.
- Merz, J. E., S. Hamilton, P. S. Bergman, and B. Cavallo. 2011. Spatial perspective for Delta Smelt: a summary of contemporary survey data. *California Fish and Game* 97:164–189.
- Miller, W. J. 2011. Revisiting assumptions that underlie estimates of proportional entrainment of Delta Smelt by state and federal water diversions from the Sacramento-San Joaquin Delta. *San Francisco Estuary and Watershed Science* 9(1):1.
- Miller, W. J., B. F. J. Manly, D. D. Murphy, D. Fullerton, and R. R. Ramey. 2012. An investigation of factors affecting the decline of Delta Smelt (*Hypomesus transpacificus*) in the Sacramento-San Joaquin Estuary. *Reviews in Fisheries Science* 20:1–19.
- Mount, J., W. Fleenor, B. Gray, B. Herbold, and W. Kimmerer. 2014. The Draft Bay-Delta Conservation Plan: assessment of environmental performance and governance. *Hastings West-Northwest Journal of Environmental Law and Policy* 20:245.
- Moyle, P. B. 2002. *Inland fishes of California*, 2nd edition. University of California Press, Berkeley.
- Moyle, P. B., B. Herbold, D. E. Stevens, and L. W. Miller. 1992. Life history and status of the Delta Smelt in the Sacramento-San Joaquin Estuary, California. *Transactions of the American Fisheries Society* 121:67–77.
- Nichols, F., J. Cloern, S. Luoma, and D. Peterson. 1986. The modification of an estuary. *Science* 231:567–573.
- Nobriga, M. L. 2002. Larval Delta Smelt diet composition and feeding incidence: environmental and ontogenetic influences. *California Fish and Game* 88:149–164.
- Nobriga, M. L., E. Loboschewsky, and F. Feyrer. 2013. Common predator, rare prey: exploring juvenile Striped Bass predation on Delta Smelt in California's San Francisco Estuary. *Transactions of the American Fisheries Society* 142:1563–1575.
- Nobriga, M., T. Sommer, F. Feyrer, and K. Fleming. 2008. Long-term trends in summertime habitat suitability for Delta Smelt, *Hypomesus transpacificus*. *San Francisco Estuary and Watershed Science* [online serial] 6(1):1.
- Orsi, J., and W. Mecum. 1986. Zooplankton distribution and abundance in the Sacramento-San Joaquin Delta in relation to certain environmental factors. *Estuaries* 9:326–339.
- Orsi, J. J., and S. Ohtsuka. 1999. Introduction of the Asian copepods *Acartiella sinensis*, *Tortanus dextrilobatus* (Copepoda: Calanoida), and *Limnithona tetraspina* (Copepoda: Cyclopoida) to the San Francisco Estuary, California, USA. *Plankton Biology and Ecology* 46:128–131.
- Orsi, J. J., and T. C. Walter. 1991. *Pseudodiaptomus forbesi* and *P. marinus* (Copepoda: Calanoida), the latest copepod immigrants to California's Sacramento-San Joaquin Estuary. Pages 553–562 in S.-I. Uye, S. Nishida, and J.-S. Ho, editors. *Proceedings of the Fourth International Conference on Copepoda*. Bulletin of the Plankton Society of Japan, Special Volume, Hiroshima.
- R Development Core Team. 2014. R: a language and environment for statistical computing. R Foundation for Statistical Computing, Vienna.
- Railsback, S. F., and B. C. Harvey. 2011. Importance of fish behaviour in modelling conservation problems: food limitation as an example. *Journal of Fish Biology* 79:1648–1662.
- Rose, K. A., W. J. Kimmerer, K. P. Edwards, and W. A. Bennett. 2013a. Individual-based modeling of Delta Smelt population dynamics in the upper San Francisco Estuary I. Model description and baseline results. *Transactions of the American Fisheries Society* 142:1238–1259.
- Rose, K. A., W. J. Kimmerer, K. P. Edwards, and W. A. Bennett. 2013b. Individual-based modeling of Delta Smelt population dynamics in the upper San Francisco Estuary II. Alternative baselines and good versus bad years. *Transactions of the American Fisheries Society* 142:1260–1272.
- Scheffer, M., J. M. Baveco, D. L. DeAngelis, K. A. Rose, and E. H. Vannes. 1995. Super-individuals a simple solution for modelling large populations on an individual basis. *Ecological Modelling* 80:161–170.
- Schreier, B. M., M. R. Baerwald, J. L. Conrad, G. Schumer, and B. May. 2016. Examination of predation on early life stage Delta Smelt in the San Francisco Estuary using DNA diet analysis. *Transactions of the American Fisheries Society* 145:723–733.
- Secor, D. H. 1999. Specifying divergent migrations in the concept of stock: the contingent hypothesis. *Fisheries Research* 43:13–34.
- Slater, S. B., and R. D. Baxter. 2014. Diet, prey selection, and body condition of age-0 Delta Smelt, *Hypomesus transpacificus*, in the upper San Francisco Estuary. *San Francisco Estuary and Watershed Science* [online serial] 12(3).
- Sommer, T., C. Armor, R. Baxter, R. Breuer, L. Brown, M. Chotkowski, S. Culbertson, F. Feyrer, M. Gingras, B. Herbold, W. Kimmerer, A. Mueller Solger, M. Nobriga, and K. Souza. 2007. The collapse of pelagic fishes in the upper San Francisco Estuary. *Fisheries* 32:270–277.
- Sommer, T., and F. Mejia. 2013. A place to call home: a synthesis of Delta Smelt habitat in the upper San Francisco Estuary. *San Francisco Estuary and Watershed Science* [online serial] 11(2):4.
- Sommer, T., F. H. Mejia, M. L. Nobriga, F. Feyrer, and L. Grimaldo. 2011. The spawning migration of Delta Smelt in the upper San Francisco Estuary. *San Francisco Estuary and Watershed Science* [online serial] 9(2):2.
- Sullivan, L. J., T. R. Ignoffo, B. Baskerville-Bridges, D. J. Ostrach, and W. J. Kimmerer. 2016. Prey selection of larval and juvenile planktivorous fish: impacts of introduced prey. *Environmental Biology of Fishes* 99:633–646.
- Thomson, J., W. Kimmerer, L. Brown, K. Newman, R. Mac Nally, W. Bennett, F. Feyrer, and E. Fleishman. 2010. Bayesian change-point analysis of abundance trends for pelagic fishes in the upper San Francisco Estuary. *Ecological Applications* 20:1431–1448.
- USFWS (U.S. Fish and Wildlife Service). 2008. Biological Opinion (BO) on the Long-Term Operational Criteria and Plan (OCAP) for coordination of the Central Valley Project and State Water Project. USFWS, California and Nevada Region, Sacramento, California.
- Walters, C., and J. Korman. 1999. Linking recruitment to trophic factors: revisiting the Beverton-Holt recruitment model from a life history and multispecies perspective. *Reviews in Fish Biology and Fisheries* 9:187–202.
- Ward, E. J., P. S. Levin, M. M. Lance, S. J. Jeffries, and A. Acevedo-Gutierrez. 2012. Integrating diet and movement data to identify hot spots of predation risk and areas of conservation concern for endangered species. *Conservation Letters* 5:37–47.
- Winder, M., and A. D. Jassby. 2011. Shifts in zooplankton community structure: implications for food web processes in the upper San Francisco Estuary. *Estuaries and Coasts* 34:675–690.

Appendix: Additional Model Details

This Appendix presents details of model structure that were reported previously (Rose et al. 2013a, 2013b) but are summarized here to enable readers to better understand model features that are particularly relevant to this paper.

Environment

The individual-based model (IBM) uses output from the Delta Simulation Hydrodynamic Model (DSM2) developed by the California Department of Water Resources (<http://baydeltaoffice.water.ca.gov/modeling/deltamodeling/models/dsm2/dsm2.cfm>). This is a one-dimensional model on a spatial grid of 517 channels and 5 reservoirs (Figure 1), which was also used as the spatial grid for the IBM. Location within each grid channel is specified in relation to X (along-channel), Y (across channel), and Z (height off the bottom) axes.

Input to DSM2 includes tidal height at a seaward boundary, freshwater inflows from the rivers, diversion flows in the south Delta, and net consumption of water within the Delta. The hydrodynamic model simulates water years 1995–2005. A water year begins on October 1 of the previous year and runs until September 30; thus, a water year includes the entire wet season and subsequent summer dry season.

The DSM2 generates hourly values of water velocity and tidal height in each channel and reservoir, which are used as inputs to a particle-tracking model (PTM) embedded in the Delta Smelt IBM. A second grid of 11 coarser boxes is overlaid onto the channel grid (Figure 1). We used long-term field data to specify daily temperature, salinity, and biomass of the six zooplankton groups (Table 1) by box for the same years as the hydrodynamic simulations. Temperature and salinity are mapped to each grid cell each day in a box by using their respective monthly means for that box, and zooplankton biomass is mapped to each cell each day by sampling from a lognormal distribution with parameters determined from historical field data for that box and month (see Appendix A in Rose et al. 2013a).

Movement

Daily movement of all individual Delta Smelt is computed as the product of the time step and their velocities in the X direction. If an individual moves past the end of a channel, it enters a node where it either continues into a new channel or enters a reservoir. The new channel or reservoir is randomly selected from all those connected to the node.

Yolk-sac larvae, larvae, and postlarvae are moved on the grid hourly by using a PTM to determine the X component of velocity (see Appendix B in Rose et al. 2013a). The PTM is a re-coded version of the PTM used in

previous studies (Kimmerer and Nobriga 2008). The PTM includes a simple representation of lateral position (Y) and distance from the bottom (Z) to allow for effects of lateral and vertical shears in velocity. The Y and Z locations are computed from random shocks to locations at the beginning of each time step.

Movement of juveniles and adults is behavioral, and their positions in the X direction only are updated every 12 h. We used a kinesis approach (Humston et al. 2004) with salinity as the cue. Kinesis represents the distance moved by each individual as the sum of an inertial component (velocity in the last time step) and a random component, with the inertial component dominating when conditions (salinity) are good and the random component dominating when conditions are poor. Kinesis is used for both short-term (every 12 h) movement and for the spawning migration to freshwater and the subsequent seaward migration of juveniles. The default movement pattern is used between May 1 and December 15 and has an optimal salinity of 2 with no bias in direction (probability of up-estuary movement is 0.5). This pattern results in a distribution in salinity space that is reasonably close to that based on catches in the estuary (Rose et al. 2013a). From December 16 to April 30, optimal salinity is set to 0 for adults, and an up-estuary bias in the direction of movement (probability of up-estuary movement is 0.85) is imposed until individuals reach freshwater. On May 1, the optimal salinity is set back to 2, and a bias to move seaward is imposed (probability of up-estuary movement is 0.15) until super-individuals reach their optimal salinity, when the movement bias is removed.

Biological Processes

Reproduction.—Each female super-individual longer than 60 mm at the start of the spawning season (first day in which temperature exceeds 12°C anywhere on the grid) is allowed to spawn up to twice in that year (Bennett 2005; Lindberg et al. 2013). Reproduction is evaluated daily. A temperature of spawning, uniformly distributed between 12°C and 20°C, is assigned to each super-individual. Once that temperature is exceeded, the spawner releases eggs at the beginning of the next 14-d tidal cycle. Fecundity is an exponential function of length. After spawning the first time, individuals may spawn a second time if (1) they have accumulated enough weight, (2) at least 14 d have passed, and (3) temperature is less than 20°C.

Each female cohort of eggs develops by a fraction of full development that depends on temperature in the box where they are spawned. Each day, the eggs that have reached full development become newly hatched yolk-sac

larvae, and the number of these is summed for each day in each box. At this point, super-individuals are created from these newly hatched larvae. Each yolk-sac larva super-individual develops at a rate determined by temperature at its location. Once yolk-sac larvae develop into larvae, they are assigned an initial length of 3 mm and continue to move passively but begin to feed exogenously.

Bioenergetics for growth.—The daily growth of each super-individual (larva through adult) is determined by a version of the Wisconsin Bioenergetics Model (Hanson et al. 1997) originally developed for Rainbow Smelt *Osmerus mordax* (Lantry and Stewart 1993) and modified with parameters suitable for Delta Smelt. Each day, weight is updated based on consumption, respiration, egestion, excretion, specific dynamic action (SDA), and—if eggs are released—losses due to reproduction as a percentage of body weight. Maximum consumption and respiration are power functions of weight, modified by a temperature-effect function; egestion is a constant fraction of consumption; and excretion and SDA are fractions of consumption minus egestion (Hanson et al. 1997). Consumption is determined each day from a functional response based on the maximum consumption rate and the biomass densities of the six zooplankton groups in the grid cell. The new weight at the end of each day is converted to length by using a length–weight relationship. Length is not allowed to decrease; length is increased only once the individual’s weight reaches its expected value based on its length (allowing for skinny fish).

Mortality.—Daily mortality includes stage-specific rates, starvation, entrainment at the two water diversion facilities (Figure 1), and old age. Stage-specific daily rates are temperature dependent for eggs (average about 0.055 per day) and constant at 0.035 per day for yolk-sac larvae (calibrated), 0.05 per day for larvae, 0.03 per day for post-larvae, 0.015 per day for juveniles, and 0.006 per day for

adults. Super-individuals are eliminated from the population through starvation if their weight falls below one-half the weight expected from their length. Entrainment mortality occurs when passive movement (larvae) or behavioral movement (juveniles and adults) places a super-individual in a grid cell corresponding to the water diversion facilities, at which point that entire super-individual is eliminated. An additional penalty is added to the daily mortality of juvenile and adult super-individuals in the South Delta box on days when net flow is negative (southward) in the Middle River (Figure 1). During calibration, this mortality factor was adjusted until the annual fraction of adults entrained—including those that arrived at the diversion facilities and those subject to this penalty—averaged about 10% over 1995–2005 (see figure 7A in Rose et al. 2013a). Total daily mortality is used to reduce the worths of the super-individuals each day. All super-individuals are removed from the model on January 1 of their third year.

Annual Population Growth

The IBM output is used to estimate a Leslie age-based matrix model for each year to summarize the highly detailed IBM results into a single variable: the annual finite population growth rate (λ). The value of λ encapsulates the detailed (daily and spatial) dynamics of the IBM, allowing for easy comparison among years and among scenarios. A 2×2 matrix model is estimated each year by computing the average maturity, fecundity, and age-specific survival rates; eigenvalue analysis is then used to determine λ (see Appendix D in Rose et al. 2013a). The λ value represents conditions from January 1 to December 31 of each calendar year. Model predictions of λ are determined only for 1995–2004 because hydrodynamic model output is missing for October–December 2005.